



Dynamic fracture of beryllium-bearing bulk metallic glass systems: A cross-technique comparison

D. Rittel ^{a,*}, A.J. Rosakis ^b

^a Faculty of Mechanical Engineering, Technion, Israel Institute of Technology, Technion City, 32000 Haifa, Israel

^b Graduate Aeronautical Laboratories, California Institute of Technology, Pasadena, CA 91125, USA

Received 31 August 2004; received in revised form 19 October 2004; accepted 19 October 2004

Available online 3 March 2005

Abstract

We report on a detailed comparison between two different experimental techniques used to measure the dynamic initiation fracture toughness K_{IC}^d of a bulk metallic glass system (Vitreloy-1) and its β -phase composite. Both the coherent gradient sensing interferometry (CGS) and one-point impact techniques reveal very similar trends in the K_{IC}^d – \dot{K}_I^d relationship for Vitreloy-1. A drastic increase in initiation toughness with the stress intensity rate is observed. By contrast, the one-point impact method shows a relative rate-insensitivity for the K_{IC}^d of the β -phase composite. The results are rationalized through a detailed characterization of the failure mechanisms.

© 2005 Elsevier Ltd. All rights reserved.

Keywords: Bulk metallic glass; Coherent gradient sensing; One-point impact; Dynamic fracture; Adiabatic shear banding

1. Introduction

The earliest studies on the mechanical properties of metallic glasses revealed their extraordinary characteristics, most notably their relatively high strength and low elastic moduli [1]. However, until recently these alloys could only be fabricated as thin sheets or rods with diameters of less than 2 mm, thereby limiting the extent of detailed experimental characterization of their mechanical properties using conventional testing techniques. The development of bulk metallic glasses by Inoue and co-workers [2,3] and Peker and Johnson [4] has heightened interest in this class of materials for a variety of engineering applications. Furthermore, the larger ingot sizes have facilitated the study of a broad range of material properties.

* Corresponding author. Tel.: +972 4829 3261; fax: +972 4832 4533.

E-mail address: merittel@technion.ac.il (D. Rittel).

Although several compositions of bulk metallic glasses have successfully been processed, one of the more promising and widely studied alloys is $\text{Zr}_{41.25}\text{Ti}_{13.75}\text{Ni}_{10}\text{Cu}_{12.75}\text{Be}_{22.5}$, also known by its commercial name, Vitreloy-1. Studies of the dynamic constitutive response of this alloy by Rosakis, Johnson and their research group have demonstrated elastic–perfectly plastic behavior with a strain-rate independent tensile/compressive flow stress of approximately 2 GPa [5,6]. Failure in these specimens occurs in a highly unstable manner along planes inclined by 45° with respect to the loading axis as a result of shear localization. Using high-speed infrared diagnostics Bruck et al. [6] observed that the temperatures accompanying localized shear failure due to adiabatic heating approach 775 K, more than 80% of the melting temperature.

Direct measurement of the static mode-I fracture toughness, K_{IC} of Vitreloy-1 has been made by Conner et al. [7] and Gilbert et al. [8] with K_{IC} of the order of $55 \text{ MPa m}^{1/2}$, a value similar to the toughness of typical high strength polycrystalline metallic alloys. However, in contrast to many steels, aluminum alloys and titanium alloys, the onset of failure is followed by highly unstable, dynamic crack propagation. A dramatic reduction in toughness has been reported when a significant fraction of crystalline phases are introduced through heating treatment [8,9], resulting in materials with $K_{\text{IC}} \sim 2 \text{ MPa m}^{1/2}$. Also Lowhaphandu and Lewandowski [10] have observed a value of $K_{\text{IC}} \sim 20 \text{ MPa m}^{1/2}$ on a nominally amorphous material of similar, but not of a composition identical to Vitreloy-1. It was suggested that this apparently lower toughness might have resulted from differences in specimen geometry or preparation or slight variations in composition.

In the studies on bulk metallic glasses cited above, dynamically propagating cracks or shear bands have been reported to occur consistently under either quasi-static or dynamic loading conditions. Although such observations have never been studied systematically thus far, these early reports indicate the importance of developing a detailed understanding of dynamic failure mechanisms in bulk metallic glasses, as well as of the transitions in failure behavior from tensile cracking to shear banding. One of the important parameters is the dynamic crack initiation toughness (K_{IC}^{d}) of these materials and its dependence on the loading rate (\dot{K}_1^{d}).

As of today, there is no standardized method to measure the dynamic initiation toughness of materials, and various methods have been suggested. Among these, the coherent gradient sensing method (CGS) is an optical method that has been devised by Rosakis [11] to obtain a full-field characterization of the crack-tip subjected to transient loading. The CGS, described in the sequel, provides a full characterization of the crack-tip throughout its history, including initiation, propagation and arrest phases. However, the method necessitates sophisticated equipment, for both optical and imaging purposes, including a costly high-speed camera with typical framing rates in excess of 1 Mfps. On the other hand, a very simple hybrid experimental–numerical approach has been devised by Weisbrod and Rittel, based on one-point impact technique [12]. These techniques will subsequently be referred to as “Caltech” and “Technion” techniques respectively. To the best of the authors’ knowledge, systematic comparisons between methods to characterize the dynamic initiation toughness have not been carried out, while such comparisons would be highly useful to the experimentalists and practicing engineers.

Consequently, the purpose of the present paper is twofold. First, two radically different methods of determination of K_{IC}^{d} are systematically compared, and as will be shown, yield identical results. The second central point of this paper is a general investigation of the dynamic initiation toughness and failure mechanisms of two grades of bulk metallic glasses, one basic and one composite. The paper is organized as follows: first, each experimental approach is described and it may be noted that the two approaches are radically different. Next, experimental results are shown for the basic BMG (Vitreloy-1), showing that identical $K_{\text{IC}}^{\text{d}}-\dot{K}_1^{\text{d}}$ trends are observed using each method. Both notch and fatigue precracked specimens are investigated and their failure mechanisms characterized. The following section reports similar results for the β -composite BMG, using the one-point impact technique [12]. The discussion section evaluates the results and establishes a comparison between the two investigated grades of BMG. The final section brings concluding remarks.

2. Experimental

2.1. Materials

Plate specimens of (w/o) $Zr_{41.25}Ti_{13.75}Ni_{10}Cu_{12.75}Be_{22.5}$ (Vitreloy-1) were provided by Amorphous Technologies International, Inc. Two different batches of material were supplied that were fabricated using varying processing parameters, the details of which are proprietary. The two batches will be designated as Lots 41 and 46, respectively. The nominal dimensions of the as-received plates were $75 \times 150 \times 4$ mm. These large plate specimens were used for the dynamic fracture experiments described below. A β -phase Vitreloy-1 composite (β -composite) of (w/o) $Zr_{56.2}Ti_{13.80}Nb_{5.0}Cu_{6.90}Ni_{5.60}Be_{12.5}$ was also supplied for investigation as small beam specimens. For each material, the dilatational and shear wave speeds of the two different materials were measured. The wave speeds, along with the measured densities were used to calculate the elastic constants of the material, as shown in Table 1.

2.2. Caltech technique

A limited number of plates were cut into smaller specimens having planar dimensions of 25×50 mm for fracture testing under quasi-static conditions which are also described below. A wire EDM notch was fabricated into the center of the longest side of the specimen, having a depth of approximately one-third of the specimen width. A fatigue crack was grown from the end of the notch using $K_{\min} = 4 \text{ MPa m}^{1/2}$ and $K_{\max} = 8 \text{ MPa m}^{1/2}$ at a frequency of 10 Hz. The extension of the fatigue crack from the end of the notch was approximately 1 mm for the smaller specimens and 2 mm for the larger specimens. The specimens were lapped and polished to provide a flat and specularly reflective surface for optical interferometry resulting in final specimen thicknesses of 3.2 ± 0.1 mm.

In the quasi-static range, $\dot{K}_I^d < 10^4 \text{ MPa m}^{1/2} \text{ s}^{-1}$, the fracture experiments were conducted in a three-point bend configuration using a hydraulic Materials Testing System. The displacement rate was varied systematically, yielding a broad range of loading rates. The time history of the stress intensity factor $K_I^d(t)$ was calculated directly from the time varying load and the specimen geometry. The fracture toughness was taken as the peak value of $K_I^d(t)$, whereas the quasi-static loading rate was determined from the slope of the $K_I^d(t)$ versus time curve, expressed as \dot{K}_I^d .

In the dynamic range, $\dot{K}_I^d \geq 10^4 \text{ MPa m}^{1/2} \text{ s}^{-1}$, a different loading configuration and diagnostic methods were used. A schematic illustration of the experimental configuration for these experiments is shown in Fig. 1. A Dynatup drop weight tower was used to load specimens in dynamic three-point bend at impact velocities ranging from 1 to 6 m/s. The mechanical fields in the vicinity of the dynamically loaded crack tip were recorded using a Cordin 330 high-speed camera in conjunction with optical interferometry. The interferometric technique employed was coherent gradient sensing (CGS) which has been described in great detail

Table 1
Physical and mechanical properties of the investigated materials

	Vitreloy-1	β -Composite
$C_l^{\text{pl}-\epsilon}$ (m/s)	5194	4576
$C_l^{\text{pl}-\sigma}$ (m/s)	4294	3813
Cs (m/s)	2429	2133
ρ (kg/m^3)	6147	6391
E (GPa)	98.7	79.9
μ (GPa)	36.3	29.1
ν	0.360	0.374

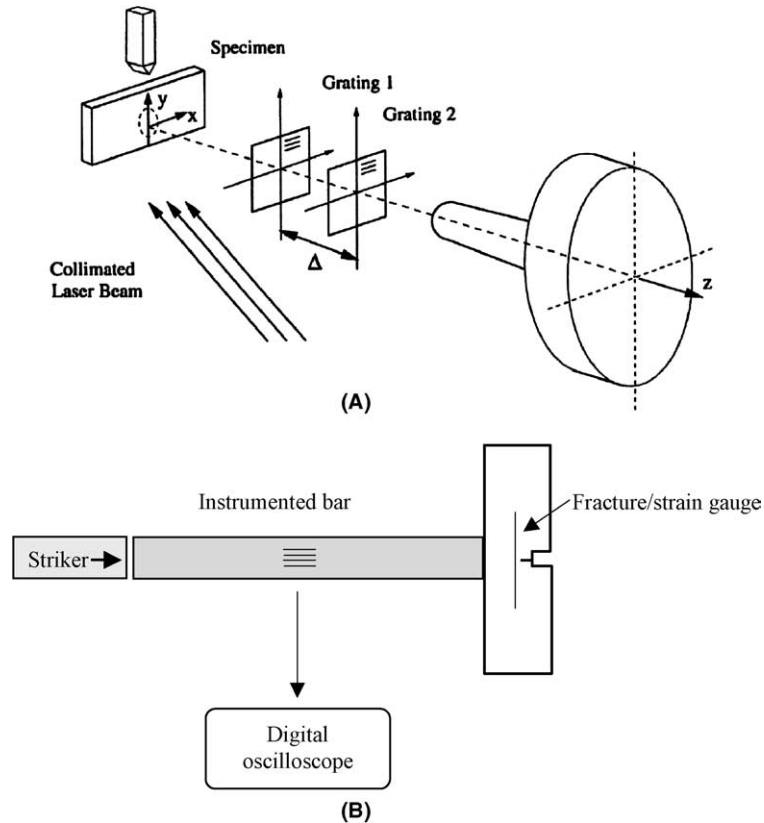


Fig. 1. (A) Experimental setup for coherent gradient sensing interferometry (CGS). (B) One-point impact setup.

elsewhere [11]. Briefly, a collimated laser beam of 50 mm in diameter was incident on the reflective specimen surface. The reflected beam, carrying information on specimen surface slopes, was processed by two gratings, G1 and G2 separated by a distance Δ . The first diffraction order was filtered using an aperture and recorded using the high-speed camera. The resulting interferograms are comprised of fringes of constant in-plane gradients of the out-of-plane displacement, u_3 . For example in Fig. 1, the crack line is parallel to the x_1 direction and the grating lines are parallel to the x_2 direction: such a configuration would yield fringes of constant $\partial u_3 / \partial x_1$. Under conditions of K_I^d dominance and plane stress, the fringe fields in polar coordinates r and θ are related to K_I^d using

$$K_I^d(t) = \left(\frac{mp}{2\Delta}\right) \left(\frac{E}{\nu h}\right) \frac{2\sqrt{2\pi r}^{2/3}}{F(\nu) \cos(3\theta/2)} \quad m = 0, \pm 1, \pm 2 \dots \quad (1)$$

where m is the fringe order, p is the pitch of the gratings (0.0254 mm), E and ν are the Young's modulus and Poisson's ratio, respectively, h is the specimen thickness and $F(\nu)$ is a known function of crack-tip speed [11]. For a stationary, dynamically loaded crack, expression (1) is still valid for $\nu = 0$. From a series of high-speed interferograms, the time history of K_I^d and the crack-tip motion history can be measured. Using this information, the values of K_I^d at crack initiation, (K_{IC}^d) and the propagation toughness, K_D associated with a given speed can be determined.

2.3. Technion technique

Short beam specimens were used, that contained two types of cracks, dividing the specimens into two equal groups: a 0.2 mm root radius notch (notched specimens), introduced either by electro-discharge machining, or using a diamond wafering blade. The other kind of specimen was fatigue precracked in three point bending (cracked specimens), using a procedure similar to that of the Caltech group. Small beam specimens, with the following dimensions were used: for the base BMG, the beam was typically 25 mm long, 4.8 mm thick and 6.1 mm high. A typical crack/notch length was 2.1 mm. For the β -composite, the beam specimen was typically 25.4 mm long, 3.0 mm thick and 10.16 mm high. A typical crack/notch length was 5 mm.

The quasi-static fracture toughness, K_{IC} , was measured in three-point bending, using an MTS 810, computer controlled servo-hydraulic testing machine. The stress intensity factor was calculated using a finite element model of the specimen, with an applied unit load of 1 N. For all tests, the load was observed to increase linearly until final abrupt fracture. Consequently, the fracture toughness was calculated by multiplying the unit SIF by the fracture load.

Based on linear elastic fracture mechanics assumptions, the transient stress intensity factor (SIF) resulting from unit impulse loading, $\hat{k}_I^d(t)$, can be calculated numerically or analytically for any cracked structure, as long as the crack remains stationary. Consequently, if the boundary conditions and applied loads $P(t)$ are well defined, the resulting stress intensity factor is given by

$$K_I^d(t) = P(t) * \hat{k}_I^d(t) \quad (2)$$

Denoting the fracture time by t_{frac} , the initiation toughness is the value of the SIF at fracture,

$$K_{IC}^d = K_I^d(t = t_{\text{frac}}) \quad (3)$$

This approach has been validated experimentally by Weisbrod and Rittel [12] using short beam specimens. These authors showed that measured crack-tip SIF's were in excellent agreement with SIF's calculated using Eq. (2). Estimation of the dynamic initiation toughness was based on Eqs. (2) and (3). The specimen was instrumented on each side with short single wire fracture gauges, whose reliability has been assessed by Weisbrod and Rittel [12], and also by Rittel and Weisbrod [13].

3. Results

3.1. Base BMG (Vitreloy-1)

The K_{IC} values measured by the Caltech group were typically $K_{IC} \approx 50 \text{ MPa m}^{1/2}$ on precracked specimens. For the notched and precracked specimen, a value of $K_{IC} \approx 56.6\text{--}77.6 \text{ MPa m}^{1/2}$ was measured at Technion, without apparent difference between the two groups. A total of two precracked and two notched specimens were used for quasi-static testing.

Dynamic fracture testing was carried out using three precracked and three notched specimens. Fig. 2 shows typical results obtained by the two techniques. Fig. 2A shows the evolution of $K_I^d(t)$, as determined using the CGS technique and crack-tip strain gauge. An excellent agreement can be noted until the onset of fracture. Typical CGS interferograms are shown in Fig. 2B. One can note the evolution the fringe pattern up to crack initiation at $t = 0.0 \mu\text{s}$. This technique allows further determination of the DSIF during the crack propagation phase. Finally, Fig. 2C shows $K_I^d(t)$ as determined using the one-point impact technique. Here too, the DSIF increases rapidly and smoothly until fracture, indicated by the single wire fracture gauges. For this technique too, it should be reminded that Weisbrod and Rittel [12] obtained excellent

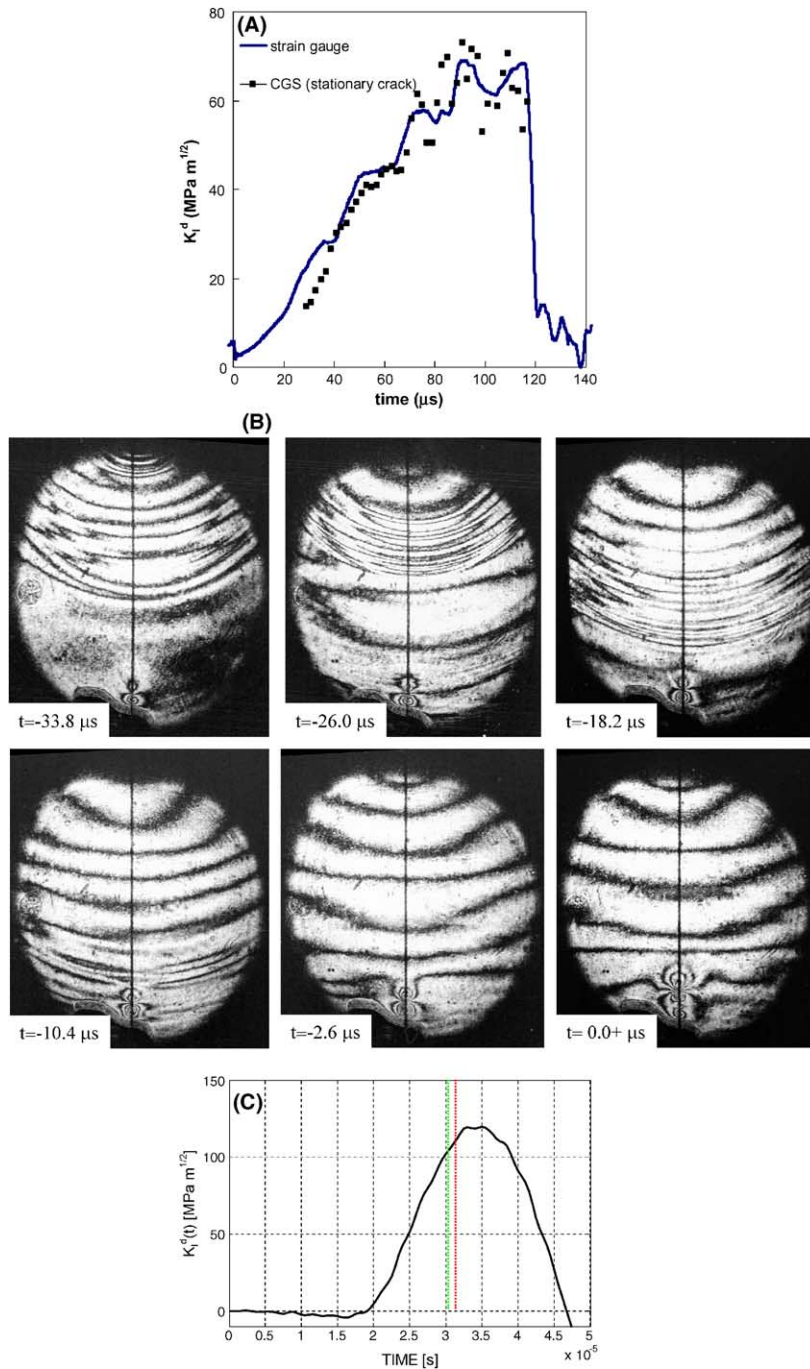


Fig. 2. (A) Typical evolution of $K_I^d(t)$ as determined using the CGS method (Caltech) and crack-tip strain gauge. Note the excellent agreement between the two methods. (B) Typical CGS interferograms. Time is counted before the onset of crack propagation ($t = 0.0 \mu\text{s}$). (C) Typical evolution of $K_I^d(t)$. One-point impact technique (Technion). Fracture time from two fracture gauges is indicated by the dashed vertical lines. Note that the evolution is not valid beyond fracture time.

agreement with crack-tip strain gauges. The values of the high-rate initiation toughness measured by each group are summarized in Table 2. Fig. 3 summarizes the $K_{IC}^d - \dot{K}_I^d$ relationship for the precracked specimens, as determined from each method. A striking similarity of the results obtained by each method is first of all noticeable. Fig. 3 also shows an identical trend for a dramatic increase in the initiation toughness with the loading rate. Fig. 4 summarizes the results obtained for notched and precracked specimens together, as tested using the short beam technique. This figure shows that the specific notches used in this work do neither influence the value of the initiation toughness nor its rate sensitivity.

Typical fracture surface morphology of quasi-statically loaded specimens is shown in Fig. 5, and of dynamically loaded specimens is shown in Fig. 6. The two main failure mechanisms are dimples and some flat cleavage-like facets. The fractographic analysis did not disclose a significant difference between the two kinds of specimens. An important point is that in all the cases, the fracture surface is essentially planar, as an extension of the fracture origin.

3.2. β -Phase composite BMG (β -phase-Vitreloy-1)

This alloy was investigated by the Technion group only. The static fracture toughness was determined from three notched and one precracked specimens. For the precracked specimen, a value of

Table 2
High rate initiation toughness values measured by the two groups

Laboratory	\dot{K}_I^d (MPa m ^{1/2} s ⁻¹)	K_{IC}^d (MPa m ^{1/2})
Caltech	2.62×10^6	179
”	5.41×10^6	160
”	5.55×10^6	286
Technion	7.41×10^6	124
Caltech	8.18×10^6	216
Technion	8.87×10^6	124
”	9.00×10^6	118

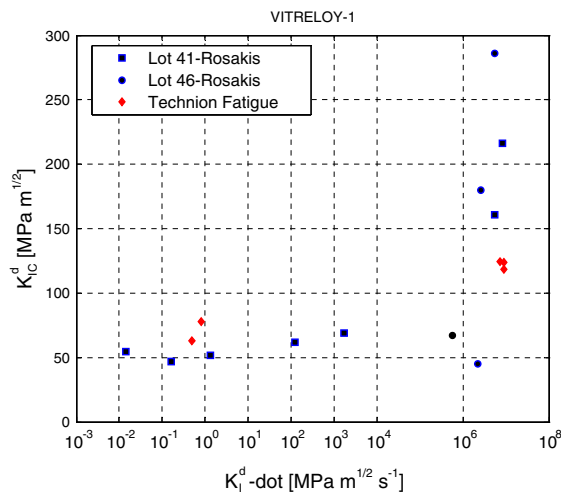


Fig. 3. $K_{IC}^d - \dot{K}_I^d$ relationship for precracked Vitreloy-1 specimens. Results obtained using the two characterization methods.

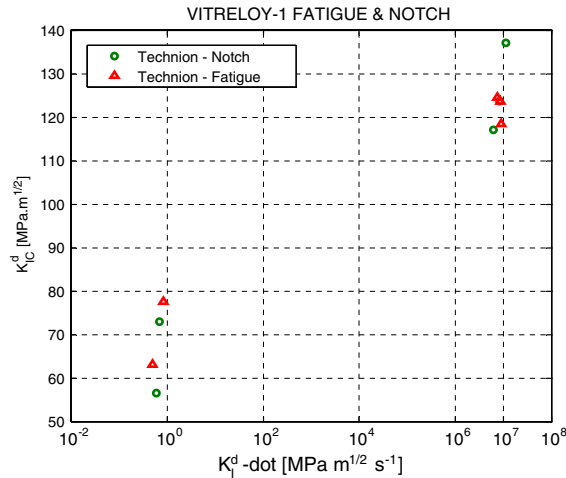


Fig. 4. K_{IC}^d – \dot{K}_I^d relationship for notched Vitreloy-1 short beam specimens. Note the relative insensitivity of the results to the crack-tip geometry.

$K_{IC} = 42 \text{ MPa m}^{1/2}$, while for the notched specimens, the initiation toughness was $K_{IC} = 92.4$ – $101.6 \text{ MPa m}^{1/2}$. In this case, the precracked specimens exhibit a significantly smaller fracture toughness than the notched specimens.

The dynamic initiation toughness was measured on six notched and four precracked specimens. Fig. 7 shows the K_{IC}^d – \dot{K}_I^d relationship for the two crack geometries. A large scatter is characteristic of the dynamic toughness of the notched specimens, while less scatter is observed for the cracked specimens. Yet, in spite of the experimental scatter, the results show that the initiation toughness of the precracked specimens is apparently insensitive to the loading rate. By contrast, the initiation toughness of the notched specimens appears to decrease at higher stress intensity rates. In addition, the initiation toughness of the notched specimens is always superior to that of the precracked specimens. In these respects, the fracture behavior of the β -composite is quite different from that of the base BMG.

The macroscopic fracture surface topography of the quasi-static beam specimens is shown in Fig. 8, while the dynamic fracture specimens are characterized in Fig. 9. These figures show that the crack initiation region of the notched specimens is comprised of teeth-like steps that form a 45° angle with respect to the fracture surface, in the crack propagation direction. By contrast, crack initiation in the precracked specimens proceeds as a smooth extension of the existing crack-tip. The presence of a tooth-like structure in the notched specimens was not observed in the base BMG. The failure micromechanisms of this material are similar to those of the base BMG, i.e. essentially dimples that reveal the ductile character of the fracture process. SEM examination of the dynamically fractured notched specimens is shown in Fig. 10. This figure clearly shows a distinct pattern of elongated dimples in the tooth-like structure, as opposed to equiaxed dimples in the planar fracture surface. Elongated dimples indicate a shear related failure mechanism, as opposed to the equiaxed dimples that indicate normal stress related failure.

4. Discussion

This work on dynamic crack initiation of beryllium bearing BMG has yielded several interesting points that will now be discussed.

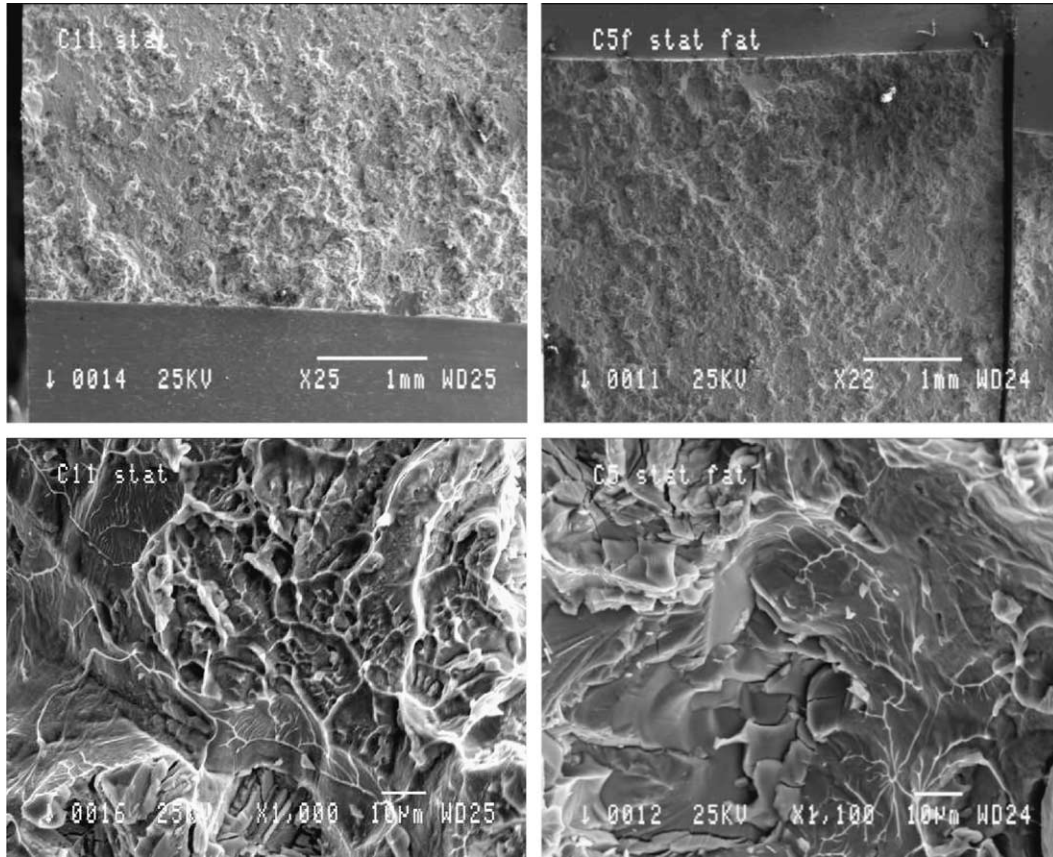


Fig. 5. Typical fracture surface morphology of notched (left column) and precracked (right column) Vitreloy-1 short beam specimens that were loaded quasi-statically. The fracture surface is planar. Failure mechanisms consist of dimples and some flat (cleavage-like) facets.

The first point concerns the methodologies used to investigate the dynamic initiation toughness. Two vastly different methods were used: a real-time full field optical method was used by the Caltech group, who applied it to relatively large notched plates. The Technion group used a hybrid experimental–numerical technique to determine the dynamic initiation toughness. Here the specimens were relatively small notched beams. For these specimens, a single term representation of the crack-tip fields was used. While the two methods were applied independently, the results were also *compared* systematically, turning the present exercise into a limited round-robin. The results point beyond any doubt to the fact that the two methods yield *very similar results*, not only in terms of initiation toughness, K_{IC} , K_{IC}^d , but also for the $K_{IC}^d - K_I^d$ relationship. However, a certain scatter can be noted in the measured toughness values. While natural scatter of this mechanical property cannot be ruled out, one should keep in mind that some experimental error is likely to be related to the identification of the onset of crack propagation. Two different approaches were used here, visual determination (Caltech) and fracture gauges (Technion). It has long been recognized that pinpointing the accurate onset of crack propagation is a delicate problem, regardless of the technique used, and the problem gets worse as the loading rate increases. Yet, to the best of the authors' knowledge, this joint exercise is the first of its kind and the trends in initiation toughness are captured by the two techniques in a very similar way. Beyond the inherent interest in the investigated material,

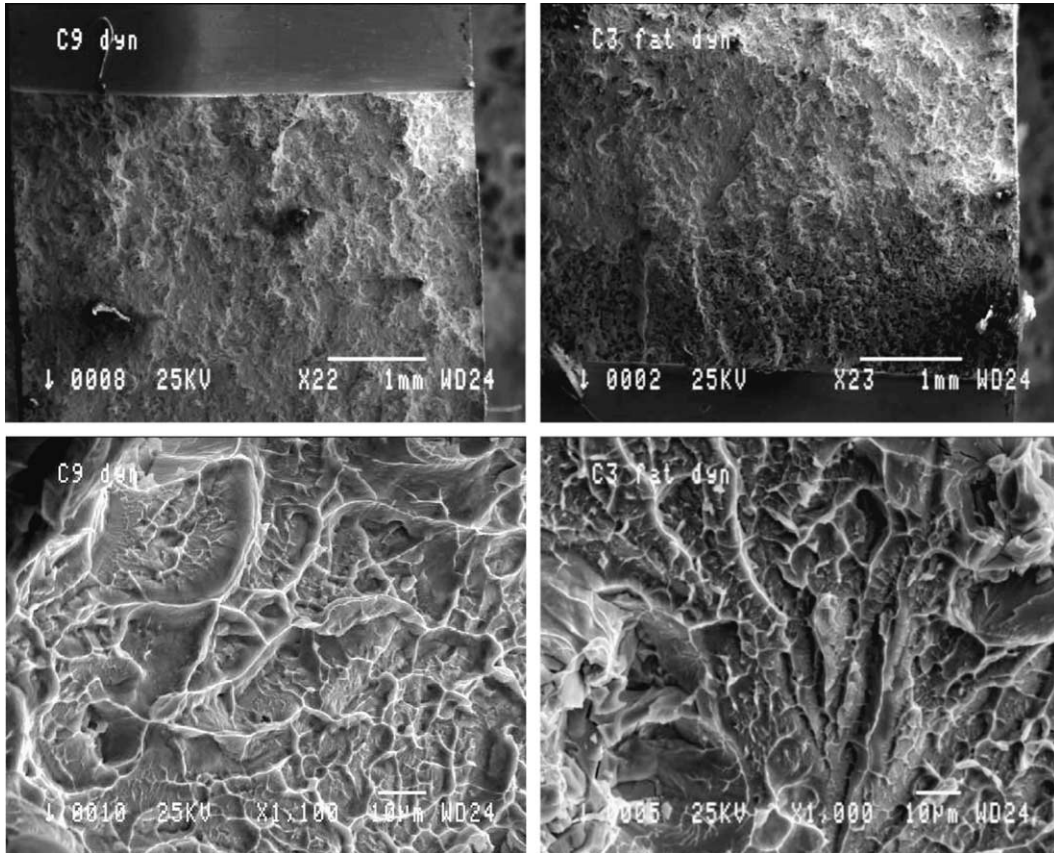


Fig. 6. Typical fracture surface morphology of notched (left column) and precracked (right column) short beam Vitreloy-1 specimens that were loaded dynamically. The fracture surface is planar. Failure mechanisms consist essentially of dimples.

the cross-comparison shows that both techniques can be reliably used to measure K_{IC}^d . The two methods are complementary, in the sense that the small beam method is quite simple to realize and yields useful information until the onset of crack initiation. By contrast, the more sophisticated CGS method overlaps with the previous one until crack initiation, but brings a wealth of useful information on the crack propagation phase, including branching and arrest. In this respect, it seems that additional similar initiatives should be encouraged to bring dynamic toughness measurements closer to the engineering realm.

The present paper also contains new and interesting results about the metallic glasses per-se. The Vitreloy-1 base metallic glass has a rate-sensitive initiation toughness. The present results are somewhat limited in the sense that there is a gap between the quasi-static and high stress intensity rates that was not covered here, but at this stage, the gap can be covered by simple interpolation technique.

The fractographic characterization does not show a specific failure micromechanism that one could incriminate for the observed toughness increase. However, looking at Zehnder and Rosakis' [14] results on the velocity dependence of AISI 4340 steel, one would note that the present K_{IC}^d – K_I^d relationship looks very similar to their K_D – V , where V is the crack-velocity. A simple explanation to the observed toughness variation lies in the fact that, following impact, the crack is initiated at a relatively high velocity, which explains the similarity between both curves. Identical rate sensitivity has been reported for a glassy polymer, PMMA [16]. For this material, the authors investigated fatigue cracks only, and reported a noticeable

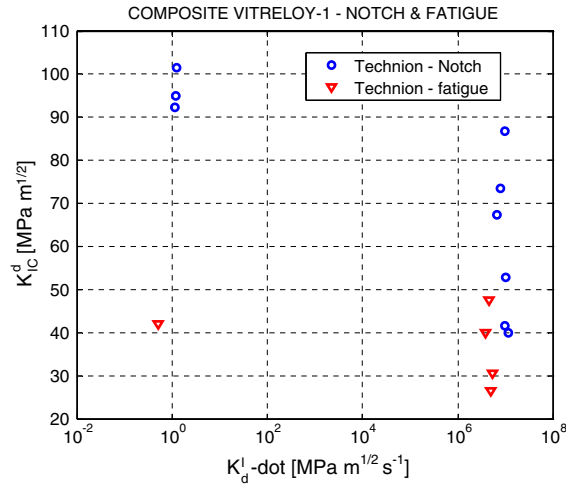


Fig. 7. $K_{IC}^d - \dot{K}_I^d$ relationship for notched and precracked β -composite specimens. Note the apparent lack of rate sensitivity of the precracked specimens, and the lower dynamic values of the notched specimens.

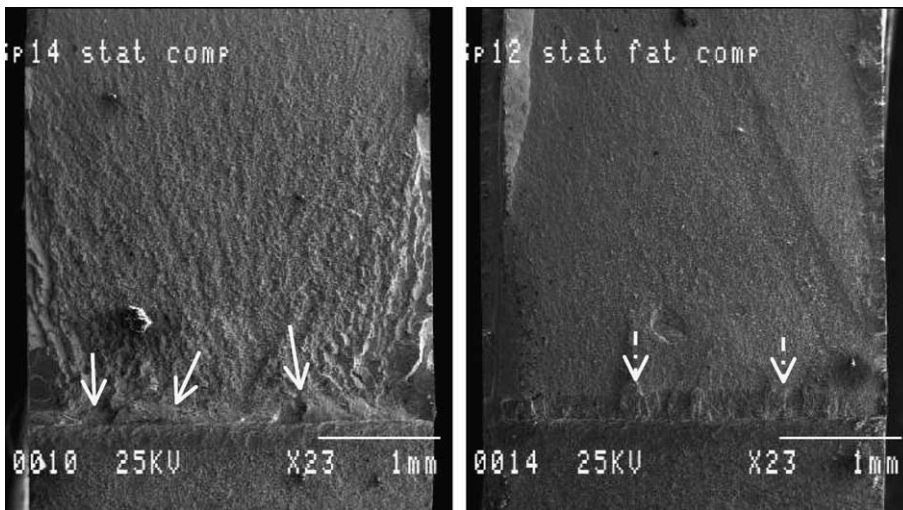


Fig. 8. Macroscopic fracture surface topography of notched (left) and precracked (right) quasi-static β -composite specimens. Note the irregular crack initiation of the notched specimen (white solid arrows). The dashed arrows point to the fatigue crack front.

increase in initiation toughness at high loading rates. This increase was explained in terms of multiple microcracks formed around the crack-tip, whose dynamic coalescence with the main crack-tip delayed the onset of crack initiation, thereby increasing the measured initiation toughness. However, a detailed roughness characterization of the fracture surface would be needed to validate this hypothesis.

An additional point is that the initiation toughness of Vitreloy-1 is apparently insensitive to the crack-tip geometry, at least in the investigated ranges. In other words, fatigue cracks and sharp notches behave identically, probably up to a certain root radius, as pointed out in early work by Malkin and Tetelman [15], who investigated the $K_{IC}^d - \sqrt{\rho}$ relationship in steels.

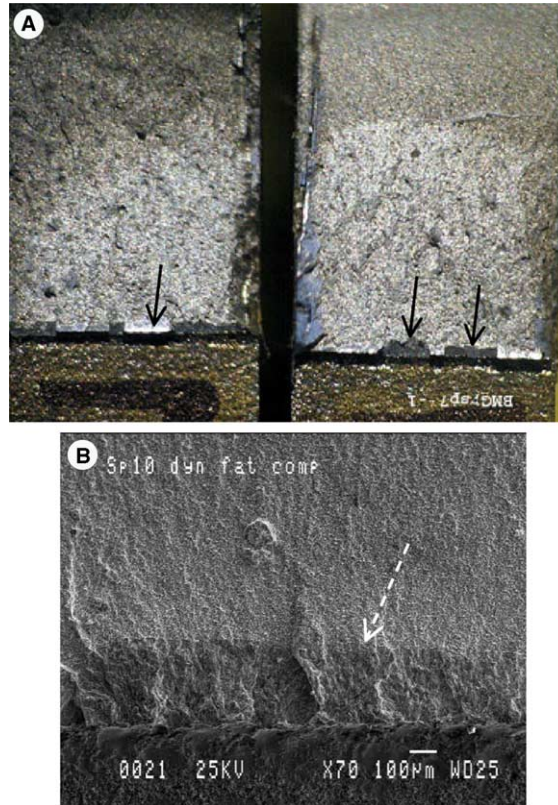


Fig. 9. Macroscopic fracture surface topography of notched (A) and precracked (B) quasi-dynamic β -composite short beam specimens. Note the irregular, teeth-like, crack initiation of the notched specimen (matching surfaces—black solid arrows). The dashed arrow points to the smooth fatigue crack front.

The present study also shows that the β -phase composite behaves quite differently. Here, one would intuitively expect an improvement of the mechanical (fracture) properties that results from the design of a composite material. Moreover, owing to the slight change in composition, one would expect the properties of the composite to somehow resemble those of the base Vitreloy-1. However, the results of the present work just point to the opposite. Firstly, the results clearly show crack (notch) geometry dependence, in the sense that the initiation toughness of notched specimens exceeds that of the precracked specimens. Whereas the precracked specimens are relatively insensitive to the stress intensity rate, the superior toughness of the notched specimens is observed to slightly decrease with the stress intensity rate. A comparison of Figs. 8 and 9 for the precracked specimens shows a relatively smooth fracture surface in both quasi-static and dynamic loading conditions, and this might explain the relative insensitivity of the initiation toughness to the stress intensity rate. The notch sensitivity is clearly correlated with the very distinctive teeth-like pattern that forms, under both quasi-static and dynamic loading conditions. This indicates a high propensity of this material for (shear) strain localization irrespective of the strain rate, i.e. (adiabatic) shear banding. The notch geometry and fracture specimen geometry have been known to influence the fracture toughness results. Lowhaphandu and Lewandowski [10] investigated a metallic glass with a composition that differs from the material investigated here. They report a marked influence of the notch root radius, which causes K_{IC} to increase from about $20 \text{ MPa m}^{1/2}$ for a precracked specimen to about $120 \text{ MPa m}^{1/2}$ for a $200 \mu\text{m}$ root radius notch. Flores and Dauskardt [17] worked on a metallic glass of identical composition to the

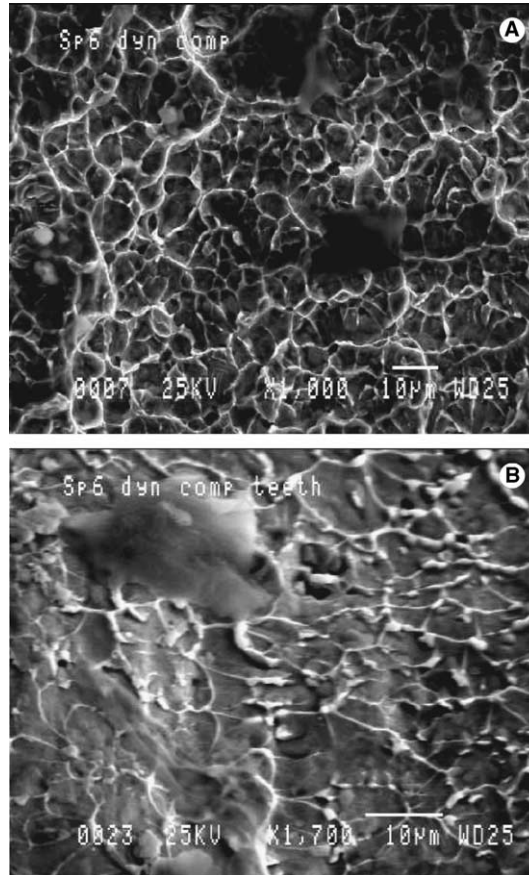


Fig. 10. Typical fracture surface morphology of a notched short beam specimen that was loaded dynamically. Failure mechanisms consist essentially of equiaxed dimples in the main fracture plane, and of elongated dimples in the teeth-like region at the origin of the crack (B).

base BMG investigated here. These authors found that the specimen geometry has a definite influence of the fracture toughness values, as a result of the slip pattern ahead of the crack (notch). When the specimen geometry involves bending, as in Lowhaphandu and Lewandowski's specimens [10], as well as in the short beam specimens, a fan-shaped slip-line pattern is expected to develop. In this case, when the material is sensitive to shear stresses (as in the case of shear localization), the crack will first develop at a 45° angle with respect to the initial crack, but after some growth, it will downturn and return to the plane of symmetry. These authors deem this crack-tip confinement effect responsible for a marked increase in fracture toughness from $\approx 55 \text{ MPa m}^{1/2}$ to $\approx 130 \text{ MPa m}^{1/2}$. The values found in the present work are in excellent agreement with those of Conner et al. [7] in spite of the geometry of the specimen used here. Indeed, when considering the composite BMG, it can be noted that the teeth-like fracture pattern that characterizes the notched specimen is quite similar to that mentioned by Flores and Dauskardt [17], to which high toughness values are associated. It also shows that, of the two investigated grades of BMG, the composite has a higher propensity to shear localization in the form of adiabatic shear banding. Bruck et al. [6], report a slant failure mechanism in axially loaded specimens in the Kolsky bar. The yield/fracture strength is of the order of 1800 MPa and it is found to be strain-rate insensitive. Such a value can now be used to estimate a mode I

SIF at the onset of shear fracture. Keeping in mind the shear banding fracture mechanism, the slight negative rate sensitivity appears to be qualitatively related to a “shear band toughness” in which adiabatic shear bands form more easily than regular quasi-static shear bands. This point requires further study.

To illustrate adiabatic shear banding, let us neglect, as a first approximation, the notch geometrical effect. The shear strength of the material is $\tau_y = 900$ MPa. The stress distribution ahead of a (static or stationary) crack is given to a first order by

$$\tau_{r\theta} = \frac{K_I}{\sqrt{2\pi r}} \sin\left(\frac{\theta}{2}\right) \cos^2\left(\frac{\theta}{2}\right) \quad (4)$$

For a typical toughness value of $K_{IC}^d = 100$ MPa m^{1/2}, a local stress equal to τ_y is reached at $r = 245$ μ m. While a more sophisticated analysis should rely on the exact solution for the stress field ahead of a notch, this value is nevertheless an indication of the distance over which the yield stress is reached (assuming a ideally-plastic material). In other words, this is also the typical size of the observed teeth, and it indeed agrees with the observations.

As a final point, it appears throughout this work that through compositional changes, the β -composite is not a simple modification of the base Vitreloy-1 BMG. It is a totally different material.

5. Conclusions

The dynamic fracture properties of Vitreloy-1 and β -composite Vitreloy-1 have been investigated. For Vitreloy-1 two different techniques of determination of the dynamic initiation toughness have been used and compared: CGS (Caltech) and one-point impact (Technion). For the composite, only one technique was employed (one-point impact), and in both cases the failure mechanisms were characterized. The following conclusions can be drawn from the present study:

- Two radically different techniques yield very similar results for the impact toughness of Vitreloy-1. This is the first round-robin of this kind and the results are very encouraging towards establishing intercomparisons between various laboratories, a point that is currently overlooked.
- Improved overall accuracy requires accurate identification of the onset of crack propagation, mostly at the high loading rates.
- The initiation toughness of Vitreloy-1 is highly rate sensitive and it increases markedly at higher stress intensity rates.
- Within the investigated range of notch/crack-tip geometries, the material is relatively insensitive to the crack/notch tip root radius.

β -Phase Vitreloy-1 composite was studied using Technion’s approach only, and the following conclusions can be drawn:

- By contrast with Vitreloy-1, the fracture toughness (both static and dynamic) of this composite material is highly dependent on the crack/notch root radius.
- The dynamic initiation toughness of precracked specimens is relatively insensitive to the stress intensity rate.
- As expected, much larger K_{IC}^d values are observed in the case of rounded notches as opposed to sharp cracks.
- However, the fracture toughness seems to decrease at higher stress intensity rates for notched specimens.

- A distinctive failure mechanism was observed to operate in notched specimens, namely the formation of shear steps (teeth-like) that form an approximate angle of 45° with respect to the fracture plane. This mechanism was neither observed in the case of precracked specimens nor in the base Vitreloy-1 material.
- The specific notch-related failure mechanisms seems to indicate a higher propensity towards shear localization (including adiabatic) in the β -composite, irrespective of the stress intensity rate, as compared with the base Vitreloy-1.
- Finally, this work shows that the two materials react in a widely different manner to dynamic crack initiation, in spite of their relative compositional similarity.

Acknowledgements

Prof. W.L. Johnson and Dr. D. Conner of Caltech are acknowledged for kindly supplying the BMG specimens and for useful discussions. D.R. acknowledges support from the Fund for Promotion of Research at Technion. AJR acknowledges support through the NSF Grant CSEM.IRG-BMG to Caltech.

References

- [1] Pampillo C. Flow and fracture in amorphous alloys. *J Mater Sci* 1975;10(7):1194–227.
- [2] Inoue A, Zhang T, Matsumoto T. Production of amorphous cylinder and sheet of La₅₅Al₂₅Ni₂₀ alloy by a metallic mold casting method. *Mater Trans Jpn Inst Met* 1990;31(5):425–8.
- [3] Zhang T, Inoue A, Matsumoto T. Amorphous Zr–Al–TM (TM = Co, Ni, Cu) alloys with significant supercooled region of over 100 K. *Mater Trans Jpn Inst Met* 1991;32(11):1005–10.
- [4] Peker A, Johnson WL. A highly processable metallic-glass—Zr₄₁.2Ti₁₃.8Cu_{12.5}Ni₁₀.0Be_{22.5}. *Appl Phys Lett* 1993;6(17):2342–4.
- [5] Bruck HA, Christman T, Rosakis AJ, Johnson WL. Quasi-static constitutive behavior of Zr₄₁.25Ti₁₃.75Ni₁₀Cu_{12.5}Be_{22.5} bulk amorphous-alloys. *Scripta Metall Mater* 1994;30(4):429–34.
- [6] Bruck HA, Rosakis AJ, Johnson WL. The dynamic compressive behavior of beryllium bearing bulk metallic glasses. *J Mater Res* 1996;11(2):503–11.
- [7] Conner RD, Rosakis AJ, Johnson WL, Owen D. Fracture toughness determination for a beryllium bulk bearing metallic glass. *Scripta Mater* 1997;37(9):1373–8.
- [8] Gilbert CJ, Ritchie RO, Johnson WL. Fracture toughness and fatigue-crack propagation in a Zr–Ti–Ni–Cu–Be bulk metallic glass. *Appl Phys Lett* 1997;71(4):476–8.
- [9] Gilbert CJ, Lippmann JM, Ritchie RO. Fatigue of a Zr–Ti–Cu–Ni–Be bulk amorphous metal: Stress/life and crack growth behavior. *Scripta Mater* 1998;38(4):537–42.
- [10] Lowhaphandu P, Lewandowski JJ. Fracture toughness and notched toughness of bulk amorphous alloy: Zr–Ti–Ni–Cu–Be. *Scripta Mater* 1998;38(12):1811–7.
- [11] Rosakis AJ. In: Epstein JS, editor. *Experimental techniques in fracture*. New York, NY: VCH Publishers Inc; 1993. p. 327–425.
- [12] Weisbrod G, Rittel D. A method for dynamic fracture toughness determination using short beams. *Int J Fract* 2000;104(1):91–104.
- [13] Rittel D, Weisbrod G. Dynamic fracture of tungsten base heavy alloys. *Int J Fract* 2001;212:87–98.
- [14] Zehnder AT, Rosakis AJ. Dynamic fracture initiation and propagation in 4340 steel under impact loading. *Int J Fract* 1990;43:271–85.
- [15] Malkin J, Tetelman AS. Relationship between K_{IC} and microscopic strength for low alloy steels. *Engng Fract Mech* 1971;3:151–67.
- [16] Rittel D, Maigre H. An investigation of dynamic crack initiation in PMMA. *Mech Mater* 1996;23(3):229–39.
- [17] Flores KM, Dauskardt RH. Enhanced toughness due to stable crack tip damage zones in bulk metallic glass. *Scripta Mater* 1999;41(9):937–43.